



ISTITUTO NAZIONALE DI FISICA NUCLEARE - ISTITUTO NAZIONALE DI FISICA NUCLEARE

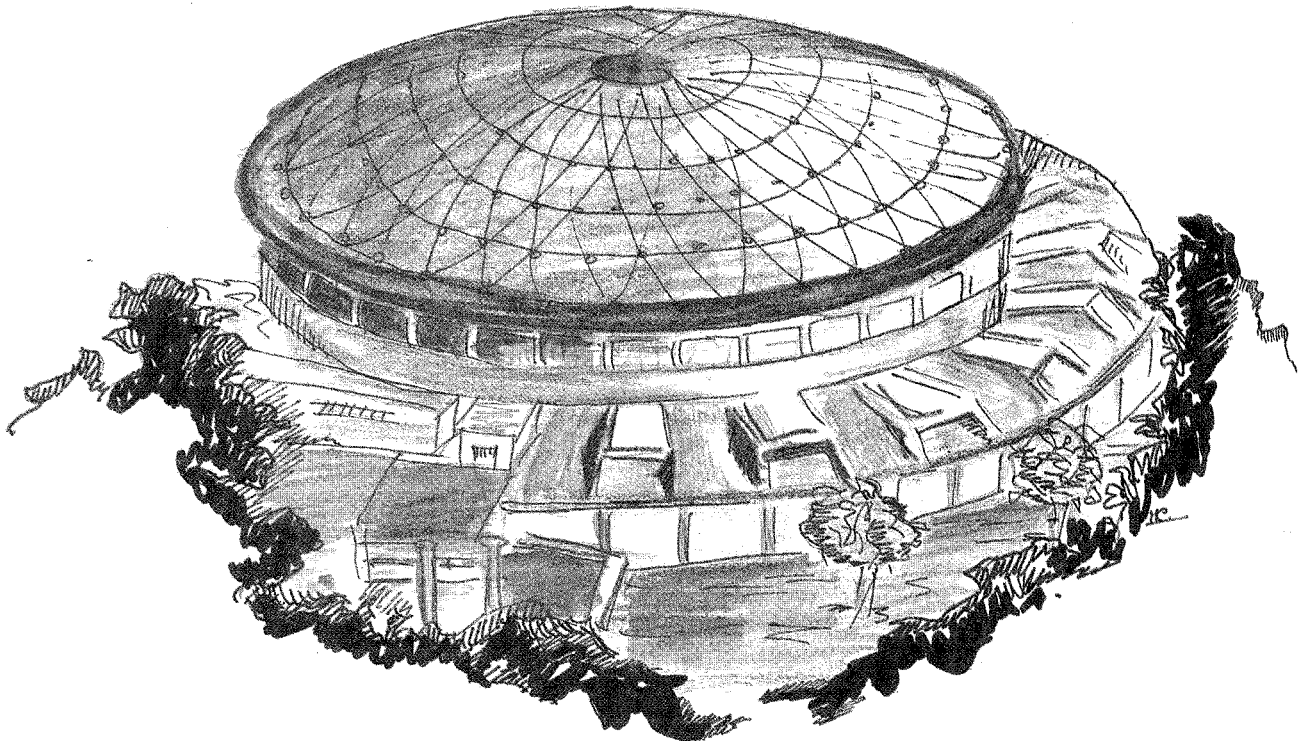
# Laboratori Nazionali di Frascati

**LNF-89/008(PT)**  
16 Febbraio 1989

E. Etim, A. Małecki and L. Satta:

## A MODEL OF DIFFRACTION SCATTERING WITH UNITARITY CORRECTIONS

Presented at the Workshop on  
"Multiparticle Dynamics"  
Perugia (Italy), June 21 -28, 1989



Servizio Documentazione  
dei Laboratori Nazionali di Frascati  
P.O. Box, 13 - 00044 Frascati (Italy)

**LNF-89/008(PT)**  
**16 Febbraio 1989**

## **A MODEL OF DIFFRACTION SCATTERING WITH UNITARITY CORRECTIONS\***

E. Etim, A. Małecki<sup>1</sup> and L. Satta<sup>2</sup>

INFN - Laboratori Nazionali di Frascati, P.O. Box 13, I-00044 Frascati (Italy)

### **1. ABSTRACT**

We note the inability of the multiple scattering model of Glauber and similar geometrical picture models to fit data at Collider energies, to fit low energy data at large momentum transfers and to explain the absence of multiple diffraction dips in the data. We argue and show that a unitarity correction to the multiple scattering amplitude gives rise to a better model and allows to fit all available data on nucleon-nucleon and nucleus-nucleus collisions at all energies and all momentum transfers. There are no multiple diffraction dips.

### **2. INTRODUCTION**

The geometrical picture of diffraction scattering comprises many phenomenological models such as the Glauber model, the Chou-Yang model, the eikonal approximation, the spectator model, etc.<sup>(1)</sup>. The idea common to these models<sup>(2)</sup> is that at very high energies a projectile has very little time, in its collision against a target, to suffer a large deviation of its path. Consequently it loses very little of its initial energy during the collision. If it traverses the target, the projectile rarely suffers multiple collisions against target constituents and is out of the target long before the changes which it induces in the target occur. These features make diffraction scattering very closely related to elastic scattering. Inelastic diffraction scattering is, in fact, sometimes referred to as quasi-elastic scattering.

---

\* Presented by E. Etim.

<sup>1</sup> On leave of absence from Institute of Nuclear Physics, 31342 Cracow, Poland.

<sup>2</sup> and Dept. of Physics, University of L'Aquila, L'Aquila, Italy.

One would expect the assumptions underlying these models to be better satisfied as the energy increases and hence for these models to provide better descriptions of the data at high energies. Experimentally<sup>(3)</sup> the opposite of these expectations are actually borne out:

- (1) Firstly the expected multiple dips in the proton-proton ( $pp$ ) and proton-antiproton ( $p\bar{p}$ ) elastic differential cross sections do not show up at the collider energies<sup>(3)</sup>.  
The first and only dip in the  $pp$  differential cross section, seen at lower energies, is less pronounced at the collider energies and tends to be less so at the higher energies. For the  $p\bar{p}$  differential cross section even this first dip is practically absent.
- (2) The observed  $pp$  and  $p\bar{p}$  elastic differential cross sections tend to be much larger than the theoretical cross sections especially for large momentum transfers where the latter are, in comparison, negligibly small<sup>(3)</sup>.
- (3) At collider energies, the measured ratio of the real to the imaginary part of the elastic scattering amplitude, in the forward direction, is relatively large (of the order of about 20%), in strong contrast with the basic assumptions of phenomenological models according to which this ratio is either zero or negligibly small<sup>(3)</sup>.

Geometrical picture models are therefore faced with a seeming paradox: a purposefully constructed high energy approximation does not work at high energies! This difficulty is not resolved by including higher and higher order multiple scattering corrections: the differences between experiment and theoretical predictions are not small and cannot therefore, be reduced by small perturbative improvements. The problem is with the geometrical approach itself. This approach is built on an analogy with optical diffraction theory (Fraunhofer diffraction) in which a target is viewed as a passive geometrical obstacle in the path of the incoming projectile. Now, at very high energies quite a lot of activity takes place inside a target through which a projectile passes and in such magnitudes that they cannot be correctly accounted for by perturbative book-keeping at the hadronic level. There is however a well known constraint which governs this activity and its consequences. It is unitarity: the opening up of a large number of multi-particle channels at high energies substantially reduces the probability for direct two-particle to two-particle scattering. These two- to -two particle scattering, including elastic scattering, are however not rare. They occur mainly through the intermediate state mediation of the large number of multi-particle states accessible kinematically. Unitarity thus has an important dynamical consequence. For instance, substantial elastic scattering is present where very little would naively be expected. This enhanced scattering is due more to the characteristic dynamics of multi-particle production than to the geometrical peculiarities of the target as an obstacle in the path of the projectile. In other words, unitarity contributions to elastic scattering from multi-particle intermediate states do not

correspond to and cannot be simulated by multiple scattering corrections of geometrical models. Consequently, multiple dips in the differential cross section, inevitable in the latter approaches, are not at all foreseen in the former because of the lack of any definite sign correlation between the various unitarity contributions.

It is proposed here to present the results of a simple model<sup>(4)</sup> of elastic scattering based on a summation over the unitarity contributions of a specific class of intermediate states. The characteristic of this class of intermediate states is that they are assumed to be "close" to the initial and final states. The intuitive idea of "closeness" is the same as implied by the concept of quasi-elastic scattering or by the quasi-degeneracy of states which differ in their contents of soft quanta. "Closeness" of states is an equivalence relation which can be made mathematically precise. This is described briefly in the next Section. In Sect. 3 we present the comparison of our results with data on a wide range of reactions: nucleus-nucleus<sup>(5)</sup> and hadron-hadron collisions<sup>(3)</sup>.

## 2. THE MODEL

Consider the S-matrix description of the scattering process  $|i\rangle \rightarrow |f\rangle$ , where  $|i\rangle$  and  $|f\rangle$  are, respectively, a given set of initial and final states. Let the S-matrix be expressed in terms of the scattering operator T as

$$S := 1 + i T \quad (1)$$

and let us operate a unitary transformation on S, which allows to present T in the form

$$T = e^{i A} T_0 e^{-i A} \quad (2)$$

By definition, A is Hermitian so that  $S_0 := 1 + i T_0$  is, like S, unitary. We now specify the transformation (2) further by requiring that  $T_0$  be a "hard" operator, more specifically, the "hard" part of T, while A describes the "soft" part in T. The theory of infra-red radiative corrections allows to understand intuitively this separation of T into "soft" and "hard" parts. Accordingly  $T_0$  is that part of T which may be calculated in QCD, perturbatively, to a certain order of the coupling constant. The soft part, on the other hand, is non-perturbative and represents the effects of the "dressing" up or hadronisation of the quark and gluon states involved in the "hard" interaction. In our approach<sup>(4)</sup> we assume that this "hard" part is given. Actually this input is a simple model Ansatz and not a QCD amplitude.

The effect of the soft part is a non-perturbative correction which we evaluate explicitly by giving the operator A suitable properties in the space of "close" states. The essential idea is that diffraction involves transitions between "close" states. Accordingly,

given a basis of physical states,  $|i\rangle, |j\rangle, |k\rangle, \dots$  we assume that  $T_0$  is diagonal in this basis, that is

$$T_0 |i\rangle = \eta_i |i\rangle \quad (3)$$

with eigenvalue  $\eta_i$ . Taking matrix elements of both sides of (2) between the states  $|i\rangle, |f\rangle$  we get

$$T_{fi} := \langle f | T | i \rangle = \sum_{k'} \eta_{k'} \langle f | e^{i A} | k' \rangle \langle k' | e^{-i A} | i \rangle \quad (4)$$

where  $|k'\rangle$  is complete set of physical states. We now approximate  $T_{fi}$  by restricting the summation over  $k'$  to only those states  $|k\rangle$  which are "close" to the state  $|i\rangle, |f\rangle$ . By assumption,  $|i\rangle$  and  $|f\rangle$  are "close", for diffractive production of  $|f\rangle$  from  $|i\rangle$ . The problem is thus reduced to the specification of the action of the operator  $A$  between any pair of "close" states. Alternatively, and more directly, one may define the concept of "closeness" in the Hilbert space of physical states with respect to the operator  $A$ . To this end, introduce the operator

$$D = \frac{1}{2} (1 - e^{i A}) \quad (5a)$$

with adjoint

$$D^\dagger = \frac{1}{2} (1 - e^{-i A}) \quad (5b)$$

and note that it satisfies the unitarity relation

$$DD^\dagger = D D^\dagger = \frac{1}{2} (D + D^\dagger) \quad (6)$$

Two states  $|j\rangle, |k\rangle$  will be said to be "close" if there exists a state  $|\lambda\rangle$  and complex functions  $\varphi_{j\lambda}$  such that<sup>(4)</sup>

$$\frac{D|j\rangle}{\varphi_{j\lambda}} = \frac{D|k\rangle}{\varphi_{k\lambda}} = D|\lambda\rangle \quad (7)$$

So defined, closeness is an equivalence relation in Hilbert space. We then say that the state  $|j\rangle$  is "close" or equivalent to the state  $|k\rangle$  modulo  $D$ , i.e.,  $|j\rangle \equiv |k\rangle \text{ mod } D$ . The equivalence classes are subspaces of the space of physical states. In fact if

$|j_1\rangle, |j_2\rangle$  are "close" and if

$$|j\rangle = C_1 |j_1\rangle + C_2 |j_2\rangle \quad (8)$$

is their linear combination with complex coefficients  $C_1, C_2$ , then one gets

$$\frac{D|j\rangle}{\varphi_j \lambda} = D|\lambda\rangle \quad (9a)$$

where

$$\varphi_j \lambda = C_1 \varphi_{j_1} \lambda + C_2 \varphi_{j_2} \lambda \quad (9b)$$

The state  $|j\rangle$  is, thus "close" to its linear components  $|j_1\rangle$  and  $|j_2\rangle$ . Generalising (8), we therefore have that the set of states

$$|\mu\rangle = \sum_{j \in \mu} C_{j\mu} |j\rangle, \quad (10)$$

formed by linear combinations of "close" states  $|j\rangle$ , forms a subspace in the space of physical states. These subspaces are the equivalence classes.

In each subspace the set of equivalent, physical states, e.g.  $|j\rangle, |k\rangle, \dots$  is therefore complete i.e.

$$\sum_{j \in \lambda} |j\rangle \langle j| = 1_\lambda \quad (11)$$

where  $1_\lambda$  stands for the unit operator in the subspace of states  $|j\rangle$  equivalent to  $|\lambda\rangle$ . Eq. (10) follows from (11). Thus putting  $|\mu\rangle \equiv |\lambda\rangle$  we find from Eqs. (10) and (11) that

$$C_{j\lambda} = \langle j | \lambda \rangle \quad (12)$$

and from Eqs. (7) and (10) for  $|\mu\rangle = |\lambda\rangle$ .

$$D|\lambda\rangle = \left( \sum_{j \in \lambda} C_{j\lambda} \varphi_{j\lambda} \right) D|\lambda\rangle \quad (13)$$

whence

$$\sum_{j \in \lambda} C_{j\lambda} \varphi_{j\lambda} = 1 \quad (14)$$

(14)

From Eqs. (11), (12) and (14) we finally get

$$\varphi_{j\lambda} = \langle \lambda | j \rangle \quad (15)$$

Multiplying Eq. (7) on the left by the bra  $| j \rangle$  and making use of the adjoint of (7) one sees that the complex number  $\lambda$  defined by

$$\lambda := \langle \lambda | D | \lambda \rangle = \frac{\langle j | D | j \rangle}{|\varphi_{j\lambda}|^2} = \frac{\langle k | D | k \rangle}{|\varphi_{j\lambda}|^2} \quad (16)$$

is an equivalence class invariant. If we now assume that the set of class representative states  $|\lambda\rangle, |\lambda'\rangle, |\lambda''\rangle, \dots$  is also complete, that is

$$\int d\mu(\lambda) |\lambda\rangle \langle \lambda| = 1 \quad (17)$$

it follows that the class representative state  $|\lambda\rangle$  is an eigenstate of  $D$  with the eigenvalue  $\lambda$ . In fact, given the state  $|\lambda\rangle$  we can expand the corresponding state  $D|\lambda\rangle$  in the  $|\lambda\rangle$ -basis to get

$$D|\lambda\rangle = \int d\mu(\lambda') \langle \lambda' | D | \lambda \rangle | \lambda' \rangle \quad (18)$$

If the state  $|\lambda\rangle$  and  $|\lambda'\rangle$  represent two inequivalent classes then the operator  $D$  should cause no transition between them, consequently

$$\langle \lambda' | D | \lambda \rangle = 0 \quad \text{if} \quad \lambda \neq \lambda' \quad (19a)$$

$$\langle \lambda' | D | \lambda \rangle = \lambda \quad \text{if} \quad \lambda = \lambda' \quad (19b)$$

Making use of (19) in Eq. (18) one gets the eigenvalue equation

$$D|\lambda\rangle = \lambda|\lambda\rangle \quad (20)$$

After this long digression we now return to Eq. (4) and substitute for  $e^{iA}$  and  $e^{-iA}$  in terms of  $D$  and  $D^*$  from Eqs. (5). Making use of the properties of physical states with respect to the operator  $D$ , Eq. (4) becomes

$$T_{fi} = \eta_i \delta_{fi} - 2\varphi_{f\lambda}^* \varphi_{i\lambda} \left[ \lambda^* \eta_f + \lambda \eta_i - 2|\lambda|^2 \eta_\lambda \right]$$

where  $\eta_\lambda$  is the average

$$\eta_\lambda := \sum_{k \in \lambda} \eta_k |\phi_{k\lambda}|^2 = \langle \lambda | T_0 | \lambda \rangle = \langle \lambda | T_0 | \lambda \rangle \quad (22)$$

Now, from Eqs. (6) and (20) one finds that the eigenvalue  $\lambda$  satisfies the unitarity<sup>(\*)</sup> condition

$$|\lambda|^2 = \operatorname{Re}(\lambda) \quad (23)$$

where  $\operatorname{Re}(\lambda)$  stands for real part of  $\lambda$ .

Making use of (23) in (21) gives

$$T_{fi} = \eta_i \delta_{fi} + 2\varphi_{i\lambda}^* \varphi_{i\lambda} \left[ i(\Delta\eta_{i\lambda} - \Delta\eta_{i\lambda}) \operatorname{Im}(\lambda) + (\Delta\eta_{i\lambda} + \Delta\eta_{i\lambda}) \operatorname{Re}(\lambda) \right] \quad (24)$$

where

$$\Delta\eta_{i\lambda} = \eta_\lambda - \eta_i \quad (25)$$

Eq. (24) achieves an enormous reduction in the task of evaluating the scattering amplitude  $T_{fi}$ : one needs the wave functions  $\varphi_{i\lambda}$  and the corresponding eigenvalues  $\lambda^{(**)}$ . By assumption, the eigen-amplitudes  $\eta_i$  of  $T_0$  in the basis of physical states are given.

$$T_{ii} = \eta_i + |2\lambda\varphi_{i\lambda}|^2 \Delta\eta_i \quad (26)$$

where we have made use of Eq. (23).

Eq. (26) is easy to apply: The first term  $\eta_i$  on its right hand side corresponds, in the geometrical picture, to totally absorptive scattering by a black disc. The second term, involving the difference

$$\Delta\eta_i = \eta_i - \eta_\lambda = \sum_{k \in \lambda} (\eta_k - \eta_i) |\phi_{k\lambda}|^2 \quad (27)$$

is a unitarity correction from intermediate scattering channels  $|k\rangle$  different from but "close" to  $|i\rangle$ . It is therefore a multi-channel correction and drastically different from the multiple scattering corrections of geometrical picture models. In other words, the second term in Eq. (26) is still available even after multiple scattering corrections to  $\eta_i$  have been made.

<sup>(\*)</sup> unitarity of  $e^{iA}$ .

<sup>(\*\*)</sup>  $\varphi_{i\lambda}^*$  are the eigenfunctions of  $D$  in the physical basis representation.

For elastic scattering, Eq. (24) reduces to Here then is the model for calculating  $T_{ii}$ : For the elastic amplitudes  $\eta_i$  we use the Glauber multiple scattering model in the impact parameter representation

$$\eta_i \equiv \eta_i(s, b, b_1 \dots b_n) = 1 - \left( 1 - \eta_{ii}(s, b) \right) \prod_{\alpha=1}^n \left( 1 - \eta_{iq}(s, b_\alpha) \right) \quad (28)$$

where it is assumed that the state  $|i\rangle$  consists of  $n$  constituents  $q_\alpha$  ( $\alpha = 1, 2, \dots, n$ ). The amplitude  $\eta_{ii}(s, b)$  corresponds to the state  $|i\rangle$  acting as a whole, that is, as if it were "elementary", whereas  $\eta_{iq}(s, b_\alpha)$  is the amplitude for the scattering of this "elementary" state against the constituent  $q_\alpha$ . The parameters  $s$  is the square of the CM energy  $\sqrt{s}$ . For the amplitudes  $\eta_{ii}(s, b)$  and  $\eta_{iq}(s, b_\alpha)$  we assume Gaussian forms

$$\eta_{ii}(s, b) = \frac{\sigma_{ii}(s)}{4 \pi a_i(s)} \exp\left(-b^2/2a_i(s)\right) \quad (29a)$$

$$\eta_{iq}(s, b_\alpha) = \frac{\sigma_{iq}(s)}{4 \pi a_q(s)} \exp\left(-b_\alpha^2/2a_q(s)\right) \quad (29b)$$

$\sigma_{ii}(s)$  and  $\sigma_{iq}(s)$  are the total cross sections for  $i-i$  and  $i-q$  scattering, respectively, with  $a_i(s)$  and  $a_q(s)$  the corresponding slopes.

Now for the states "close" to or equivalent to the state  $|i\rangle$  we take all those states  $|i, n_q\rangle$  ( $n=0, 1, 2, \dots$ ) differing by the number of constituents  $q_\alpha$ . For  $n=0$  we have what was referred to as the "elementary" state  $|i\rangle$  above. For the wave functions of these states we take

$$|\psi_{i\lambda}|^2 = |\phi_{in}(b_1 \dots b_n)|^2 = P_n \prod_{\alpha=1}^n |\psi(b_\alpha)|^2 \quad (30a)$$

$$\psi(b) = \frac{1}{\sqrt{2\pi R_0(s)}} \exp\left(-b^2/4R_0(s)\right) \quad (30b)$$

where  $R_0$  is a free parameter and  $P_n$  the probability distribution of the  $n$  constituents.  $P_n$  is assumed to be a Poisson distribution, for simplicity, i.e.

$$P_n = e^{-\bar{n}} \frac{(\bar{n})^n}{n!} \quad (31)$$

Going back to Eq. (26), one sees that it remains only to specify the eigenvalue  $\lambda$  in order for  $T_{ii}$  to be fully determined by Eqs. (26), (28) - (31). We leave  $\lambda$  as a free parameter to be fitted to experiment. Substituting from Eqs. (28) - (31) into (26) and taking Fourier transform, one finds

$$\frac{d\sigma_i(s,t)}{dt} = \pi |T_{iG}(s,t)|^2 \quad (32a)$$

$$T_{iG}(s,t) = \int_0^\infty db b J_0(b \sqrt{|t|}) T_{iG}(s,b) \quad (32b)$$

$$T_{iG}(s,b) = \eta_{ii}(s,b) + |2\lambda|^2 (1 - \eta_{ii}(s,b)) . (1 - e^{-h_i G(s,b)}) \quad (32c)$$

and

$$h_{iG}(s,b) = \frac{\bar{n} \sigma_{iq}(s)}{4\pi R(s)} \exp(-b^2/2R(s)) \quad (33a)$$

$$R(s) = R_0(s) + a_q(s) \quad (33b)$$

$T_{iG}(s,t)$  stands for the amplitude obtained from the Glauber model as input for the elastic eigen-amplitudes  $\eta_i(s, b, b_1, \dots b_n)$ . The first term  $\eta_{ii}(s, b)$  in Eq. (32c) corresponds to scattering from a black disc. Note that  $i T_{iG}(s,t)$  is purely imaginary according to Eqs. (32b) and (32c). It would make no difference if the right hand side of Eq. (31b) were normalised so that  $T_{iG}(s,t)$  is purely real. The important fact is that in either case the amplitude so defined is not analytic and, consequently, not consistent with unitarity. The latter circumstance could be tolerated in multiple scattering models but not in the present approach which is based explicitly on multi-channel dynamics and unitarity. This problem is not solved in this paper, at least, not with an analytic function. The complexification of the amplitude is achieved by using separate approximations for the real and imaginary parts. The real part is assumed to be dominant at large momentum transfers while the imaginary part dominates at small momentum transfers. The real part is assumed to be given by the Chou-Yang model<sup>(6)</sup> within the same geometrical picture scheme. The amplitude, in impact parameter space, is given by

$$T_{iCY}(s, b) = 1 - e^{-h_{iCY}(s, b)} \quad (34a)$$

$$h_{CY}(s, b) = \frac{\bar{n} \sigma_{iq}(s)}{4\pi} \frac{\mu^2}{48} (\mu b)^3 K_3(\mu b) \quad (34b)$$

where we have used a dipole  $F_i(t) = (1 + |t|/\mu)^{-2}$  for the form factor of the  $|i\rangle$  state. Comparing (34a) with (32b) one notices the absence of the scattering from a black disc. The complete scattering amplitude is thus

$$T_i(s, t) = i \cdot \int_0^\infty d b b J_0(b \sqrt{|t|}) T_i(s, b) \quad (35a)$$

$$T_i(s, b) = T_{iG}(s, b) - i T_{iCY}(s, b) \quad (35b)$$

$T_i(s, t)$  is not an analytic function. The rationale behind Eq. (35) is the following: separately, the Glauber and Chou-Yang models fit the data in the near forward direction and each quickly leads to multiple diffraction dips as  $t$  increases. The multiple dip structures are not present in the data. Eq. (35) gives a possibility for eliminating these multiple dips. Since the dip structures of  $T_{iG}(s, t)$  and  $T_{iCY}(s, t)$  are unrelated, they tend, generally, to cancel each other out. This is the more so since (in our procedure)  $T_{iG}(s, t)$  is large where  $T_{iCY}(s, t)$  is small and vice versa.

### 3. COMPARISON WITH DATA

The model described in the last section is compared with data on nucleon-nucleon and nucleus-nucleus scattering in this section. Figs. 1 give this comparison for proton-proton ( $pp$ ) and proton-antiproton ( $p\bar{p}$ ) elastic scattering. Table I gives the values of the parameters used. In Figs. 2 we compare the model with data on  $\alpha N \rightarrow \alpha N$  scattering with  $N = \alpha, d, {}^3\text{He}$ . Table (II) gives the values of the corresponding parameters in the fits. Finally in Figs. (3a) – (3c) we compare the model with deuteron-deuteron ( $dd$ ) scattering. This is a notoriously recalcitrant case which has not been amenable to model treatments. Table III gives the values of the parameters used.

Our first comment on these fits is that, unlike for other models, they extend over a wide range of momentum transfers  $0 \leq |t| \leq 10 \text{ GeV}^2$ , and energies,  $0 \leq \sqrt{s} \leq 600 \text{ GeV}$ . Secondly a detailed knowledge of the (ground state) wave functions of the scattering states is not required. The usual Gaussian wave function in impact parameter space is sufficient for our purposes. This is true also for the deuteron for which, because of its spin one

character, it was supposed that an admixture of S and D waves was required to fit the data. As Figs. (3a) - (3c) show this detail is unnecessary. What really matters is the unitarity improvement of the multiple scattering scheme. This is the more important because it allows to fit the data over so wide a range of momentum transfers despite the simplifying assumptions involved.

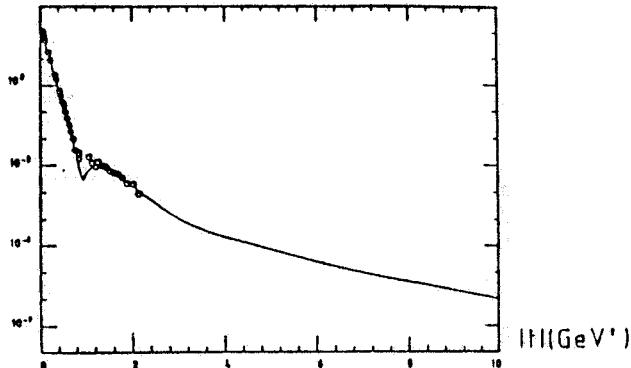


FIG. 1a -  $\bar{pp}$  differential cross section at  $\sqrt{s}=546-630$  GeV. The data are from Ref. (3a).

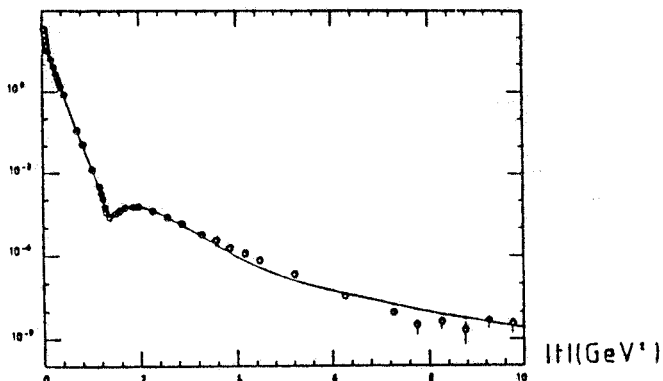
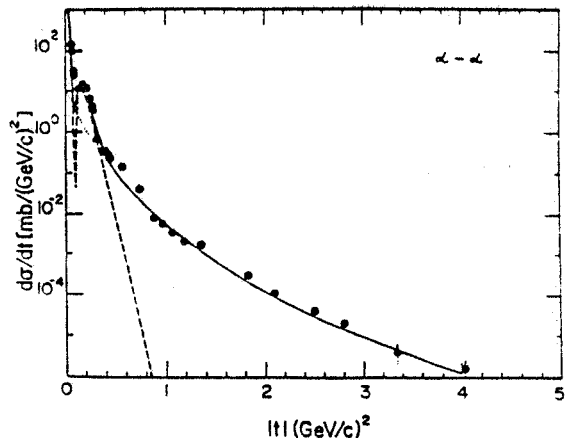


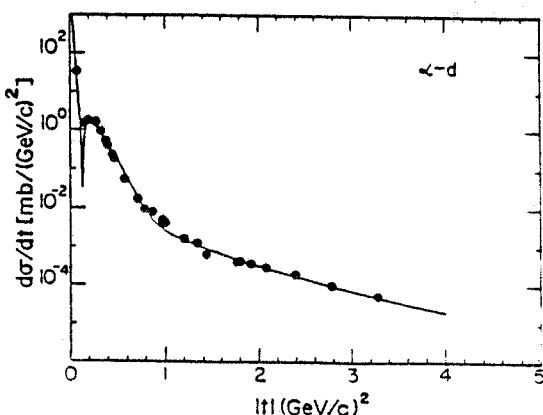
FIG. 1b -  $\bar{pp}$  differential cross section at  $\sqrt{s}=53$  GeV. The data are from Ref. (3a).

TABLE I - Values of the parameters used in the fits in Figs. 1. G stands for Glauber amplitude and CY for the Chou-Yang amplitude.

$\sqrt{s}$ (GeV)	$\sigma_{pp}$ (mb)	$a_p$ (fm) $^2$	$ \lambda ^2$	R (fm) $^2$	$\mu$ (GeV)	G	$\sigma_q$ (mb)	C-Y
53	39.3	0.49	41.0	0.17	1.648		0.034	0.110
546	53.7	0.66	41.2	0.24	1.633		0.107	0.245



**FIG. 2a** - The model is compared with  $\alpha\alpha$  elastic scattering data (full line). Dashed line: Glauber contribution. Dotted line: Chou-Yang contribution. Data are from Ref. (5b).



**FIG. 2b** - Results of the model for  $\alpha d$  elastic scattering. Data from Ref. (5b).

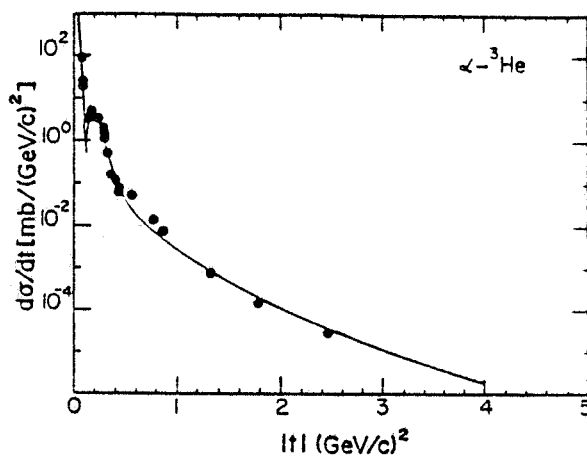


**FIG. 2c** - Same as Fig. 2b, but for  $\alpha - {}^3\text{He}$  elastic scattering. Data from Ref. (5b).

**TABLE II** - Values of the parameters used in the fits.

	$ \lambda ^2$	$a_{\alpha N}$	$\sigma_{\alpha N}$	R	$\sigma_q$	$ \lambda ^2 \sigma_q$	$\mu$
		(GeV/c) <sup>-2</sup>	mb	(GeV/c) <sup>-2</sup>	mb	mb	GeV
$\alpha d$	87	66	381	33	1.1	96	1.7
$\alpha {}^3\text{He}$	63	46	384	95	2.8	176	1.1
$\alpha\alpha$	55	49	203	96	8.3	456	0.8

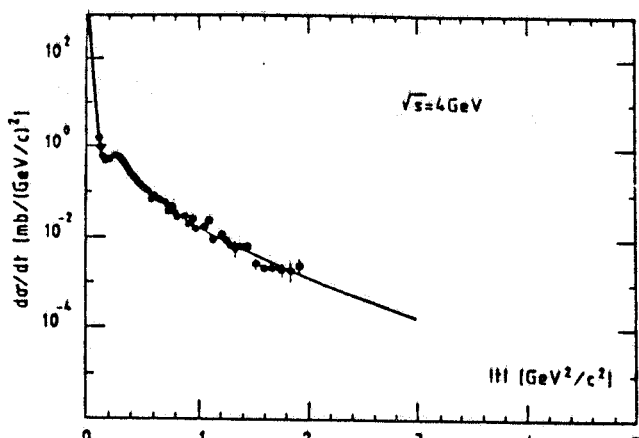


**FIG. 3a** - Plot of d-d elastic differential cross section  $d\sigma(s,t)/dt$  against  $t$  for CM energy  $\sqrt{s}=4 \text{ GeV}$ . The data points are from Ref. (5a).

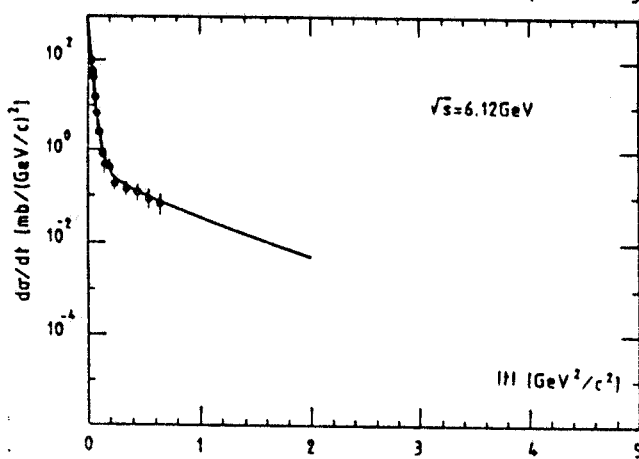


**FIG. 3b** - Same as in Fig. 3a, for  $\sqrt{s}=6.12 \text{ GeV}$  and data points from Ref. (5b).

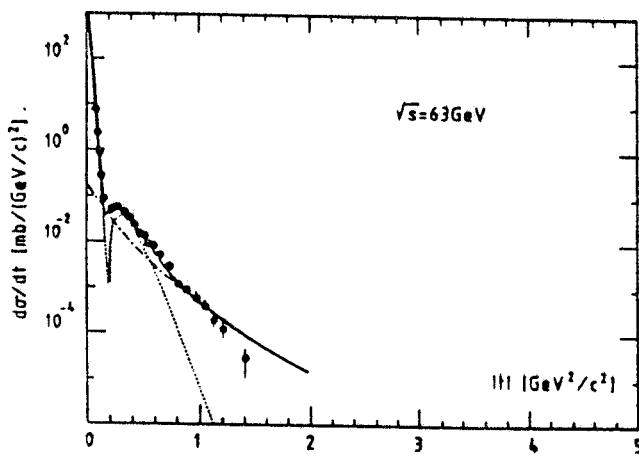


**FIG. 3c** - Same as in Fig. 3a, for  $\sqrt{s}=6.3 \text{ GeV}$  and data points from Ref. (5c).

**TABLE III** - Values of the parameters used in the fits.

$\sqrt{s}$ (GeV)	$ \lambda ^2$	$a_{dd}$ ( $\text{GeV}/c$ ) $^{-2}$	$\sigma_{dd}$ (mb)	$R$ ( $\text{GeV}/c$ ) $^{-2}$	$\sigma_q$ (mb)	$ \lambda ^2 \sigma_q$ (mb)	$m$ (GeV)
4	113	128	559	44	2.2	249	1.24
6.12	84	1451	618	99	1.3	112	1.56
63	90	104	450	39	0.96	86	0.938

**REFERENCES**

- (1) For a comprehensive review see the Reprint volume; Geometrical Pictures in Hadronic collisions; Ed. S.Y. Lo (World Scientific Publishing Co. Pte. Ltd., Singapore, 1987).
- (2) R. Glauber; Lectures in Theoretical Physics, Vol. 1, Eds. W.E. Brittin and L.G. Dunham (Interscience, New York, 1959) pp 315-414.
- (3) a) M. Bozzo, et al.; Phys. Lett. **B147** (1984) 385; **B155** (1985).  
b) A. Breakstone et al.; Nucl. Phys. **B248** (1984) 253.  
c) UA4 Collaboration; D. Bernard et al., Phys. Letts. **B171** (1986) 142.
- (4) E. Etim, A. Malecki and L. Satta; Phys. Letts. **B184** (1987) 99; E. Etim and A. Malecki; Nuovo Cimento A (to appear) and Frascati Report LNF-86/45 (1986); E. Etim and L. Satta; Nuovo Cimento A (to appear) and Frascati Report LNF-87/17 (1987); E. Etim and L. Satta; Nuovo Cimento A (to appear) and Frascati Report LNF-88/44 (1988).
- (5) a) J.V. Allaby et al.; Nucl. Phys. **B52** (1973) 316;  
b) L. Satta et al.; Phys. Letts. **B139** (1984) 263;  
c) E. T. Whipple et al.; Phys. Rev. Letts. **47** (1988) 774;  
d) A. T. Goshaw et al.; Phys. Rev. Letts. **25** (1970) 249;  
e) G. Goggi et al.; Nucl. Phys. **B149** (1979) 381;  
f) K. R. Shubert; Tables of Nucleon-Nucleon Scattering, in: Landolt-Börnstein, Numerical Data and Functional Relationship in Science and Technology, New Series, Vol. 1/9a (1979).
- (6) T.T. Chou and C.N. Yang; Phys. Rev. **170** (1968) 1591; Phys. Rev. **D19** (1979) 3268; Phys. Letts. **B128** (1983) 457.